PHYSICAL REVIEW B VOLUME 12, NUMBER 7 1 OCTOBER 1975

Itinerant-electron ferromagnetism in $La_{1-x}Sr_xCoO_3$: A Mössbauer study

V. G. Bhide and D. S. Rajoria
National Physical Laboratory, New Delhi 110012, India

C. N. R. Rao, G. Rama Rao, and V. G. Jadhao
Indian Institute of Technology, Kanpur 208016, India

(Received 25 June 1974)

Mössbauer and other studies establish that in $La_{1-x}Sr_xCoO_3$ ($x > 0.125$), ferromagnetic Sr^{2+}-rich clusters coexist with paramagnetic La^{3+}-rich regions in the same crystallographic phase, with the ferromagnetic component increasing with increasing x and decreasing T. The $3d$ holes created by Sr^{2+} substitution are itinerant both above and below T_C. All the experimental observations on this system can be explained on the basis of itinerant-electron ferromagnetism.

I. INTRODUCTION

A detailed study of $LaCoO_3$ employing Mössbauer spectroscopy as well as magnetic, electrical, and other measurements was reported by us recently.[1] In $LaCoO_3$, all the cobalt ions are in the diamagnetic low-spin configuration at very low temperatures. The low-spin $Co^{III}(t_{2g}^6 e_g^0, {}^1A_{1g})$ is, however, more stable with respect to the high-spin $Co^{3+}(t_{2g}^4 e_g^2, {}^5T_{2g})$ only by about 0.05 eV. With increase in temperature, the Co^{III} ions transform to Co^{3+} ions and the inverse magnetic susceptibility versus temperature curve shows a plateau in the 400–650-K region owing to short-range ordering.[2] Raccah and Goodenough[2] identified a symmetry change from $R\bar{3}c$ to $R\bar{3}$ after this ordering and also observed a transition due to the delocalization of the e_g electrons (localized at lower temperatures at high-spin Co^{3+} ions) to σ^*-band electrons at 1210 K. Beyond this $e_g \rightarrow \sigma^*$ transition, $LaCoO_3$ becomes metallic. Our Mössbauer studies[1] on $LaCoO_3$ established the evolution with temperature of Co^{3+} ions up to 200 K beyond which there was electron transfer between the two cobalt ions giving rise to intermediate-spin tetravalent $Co(t_{2g}^4 e_g^1)$ and $Co^{II}(t_{2g}^6 e_g^1)$ ions.[3] The population of Co^{3+} exceeded 50% below the $R\bar{3}c \rightarrow R\bar{3}$ transition temperature (650 K) so that the driving force for the development of unique cobalt sites could be due to the onset of electron transfer. Our studies also showed that Co^{3+} completely disappears at the localized-itinerant-electron transition ($e_g \rightarrow \sigma^*$) at 1210 K. In this paper, we report a detailed investigation of the novel oxide system $La_{1-x}Sr_xCoO_3$, $0 < x \leq 0.5$, the end number ($x = 0$) of which is $LaCoO_3$.

Jonker and Van Santen[4] first showed that the system $La_{1-x}Sr_xCoO_3$ becomes ferromagnetic for $x > 0.15$ and associated the ferromagnetism with the concentration of tetravalent cobalt which increases with Sr^{2+} concentration. The paramagnetic susceptibility of these solids could be explained by the Curie-Weiss law with Θ changing from a negative to a positive value around $x = 0.15$. However, the magnitude of magnetization and paramagnetic Curie temperatures could not be reconciled with the then existing theory. Goodenough,[5] assuming the $3d$ electrons to be localized, interpreted the ferromagnetism by modifying the superexchange model of Anderson.[6] According to Goodenough, a 180°K superexchange interaction $Co^{3+}(t_{2g}^4 e_g^2)$-O^{2-}-$Co^{IV}(t_{2g}^5 e_g^0)$ would be ferromagnetic. However, Goodenough[7] has later pointed out that covalent mixing between the transition-metal d orbitals and oxygen $2p$ orbitals may enhance the superexchange interaction sufficiently to break down the conditions for localized d electrons. It is now known that delocalization of d electrons is much more prevalent in transition-metal oxides, particularly in those with perovskite structure, than suspected earlier.[7,8] Studies on $LaCoO_3$ referred to earlier[1,2] clearly bring out the localized versus collective behavior of the d electrons in such oxides. Studies on $La_{1-x}Sr_xCoO_3$ by Raccah and Goodenough[9] showed that the $e_g \rightarrow \sigma^*$ transition of $LaCoO_3$ persists to relatively high values of x, the enthalpy change decreasing with x as expected for a two-phase mixture, although they found no crystallographic evidence for two phases. At $x \approx 0.5$, the solid becomes metallic. These observations led Raccah and Goodenough[9] to the conjecture that whereas all the electrons in the σ-bonding orbitals are delocalized at the highest temperature; at low temperatures, some of the electrons get trapped as localized e_g electrons at Co^{3+} ions in the La^{3+}-rich regions. They also associated the ferromagnetism in $La_{1-x}Sr_xCoO_3$ with the Sr^{2+}-rich regions and paramagnetism with the La^{3+}-rich regions. The present study was undertaken to elucidate

clearly the various conceptual problems raised by the $La_{1-x}Sr_xCoO_3$ system which exhibits both ferromagnetism and itinerant-electron behavior at large x.

We have employed temperature-dependent Mössbauer spectra to obtain direct evidence for localized versus itinerant d electrons in the ferromagnetic phase as well as for the formation of interpenetrating ferromagnetic and paramagnetic clusters within a single crystallographic phase. In addition, we have used x-ray diffraction for structural studies, differential thermal analysis for the study of phase transitions, reflectance spectra to examine plasma oscillations, and electrical-resistivity and Seebeck-coefficient measurements for electron-transport studies. Although some of the measurements, with the exception of the Mössbauer studies, have been reported by other workers, we believe that it is important to have a systematic study of all the properties on the same samples. These additional measurements have helped to confirm our chemical analysis and have provided information complementary to that yielded by Mössbauer spectroscopy.

We find that for $x \leq 0.1$ the behavior of $La_{1-x}Sr_xCoO_3$ is similar to that of $LaCoO_3$. These compositions show a plateau (although of decreasing width with increasing x) in the reciprocal magnetic susceptibility χ^{-1} versus T curve, a first-order transition from localized-electron to collective-electron behavior at about 1210 K, and two resolved Mössbauer paramagnetic peaks down to 78 K corresponding to high-spin trivalent iron and low-spin trivalent iron and/or tetravalent iron (arising out of corresponding cobalt ions in the sample). At $x \approx 0.125$, a discontinuity in lattice parameter versus x is correlated with a change in the Mössbauer spectra. For compositions $x > 0.125$, the Mössbauer spectra at lower temperatures show a magnetically split spectrum against the background of a paramagnetic spectrum. The magnetically split spectrum disappears at the respective Curie temperature. The ratio of paramagnetic to ferromagnetic signal increases with decreasing x and with increasing temperature, showing unequivocally the existence of the postulated ferromagnetic clusters in a paramagnetic matrix. The hyperfine field and the isomer shift indicated by the magnetically split spectrum lies in between those characteristic of high-spin trivalent iron Fe^{3+} and low-spin tetravalent iron Fe^{IV} (arising out of the electron-capture decay of high-spin trivalent cobalt and low-spin tetravalent cobalt ions, respectively, in the sample). This demonstrates that the electrons responsible for the electronic conductivity are itinerant. The single paramagnetic peak above T_C with an isomer shift lying in between that characteristic of Fe^{3+} and Fe^{IV} show that a similar situation prevails in the paramagnetic state as well. These findings are consistent with a metallic magnitude and temperature coefficient of the electrical resistivity and Seebeck coefficient. Thus Goodenough's conjecture of the existence of itinerant-electron ferromagnetism and of interpenetrating ferromagnetic and paramagnetic domains at intermediate values of x and low temperature appear to be established.

II. EXPERIMENTAL

Samples of $La_{1-x}Sr_xCoO_3$ with various values of x were prepared by coprecipitating the oxalates in the required proportions, essentially following the method described earlier.[1,10] The mixture of oxalates was first ground and then slowly decomposed at 870 K. The resulting mixture was ground thoroughly, made into dense thick pellets, and heated at 1200 K for 24 h. The resulting product was again ground, made into dense pellets, and fired at 1450 K for 24 h. One of the $La_{0.5}Sr_{0.5}CoO_3$ samples, prepared by P. M. Raccah, was obtained through the kind courtesy of J. B. Goodenough. The $La_{0.5}Sr_{0.5}CoO_3$ samples had a golden-brown bronze color and a density that approached 95% of the theoretical value. All the samples were checked for stoichiometry by using thermogravimetry.

The x-ray patterns for the various compositions were obtained using a General Electric XRD-6 diffractometer. The differential-thermal-analysis (DTA) studies were made using an Aminco thermoanalyzer. Electrical-resistivity measurements were carried out employing the four-probe technique, and Seebeck-coefficient measurements were made with respect to platinum. Reflectance spectra were recorded with respect to magnesium carbonate, employing a Beckman spectrophotometer.

For Mössbauer spectroscopy, these samples were used as sources. The radioactive source was prepared by evaporating a few drops of an aqueous solution of $^{57}CoCl_2$ from the pellets of various compositions $La_{1-x}Sr_xCoO_3$. ^{57}Co was thermally diffused into the lattice around 1100 K for nearly 2 h. After thermal diffusion of ^{57}Co, the sample was cooled slowly to room temperature. The surface activity was scraped off, and then the samples were used as Mössbauer sources. In a few samples, ^{57}Co was incorporated into the oxalates themselves before synthesizing the compounds.

$La_{1-x}Sr_xCoO_3$:^{57}Co sources were matched against an enriched (to 90%) type-310 stainless-steel (310 ESS) absorber over a temperature range 78–1200 K. The 310-ESS absorber, when matched against

a Cu:^{57}Co source, gave a single line with a linewidth of 0.70± 0.02 mm/sec. In some cases, the sources were matched against a $K_4Fe(CN)_6 \cdot 3H_2O$ single-crystal absorber. With a standard source, this absorber gives a linewidth of 0.28± 0.02 mm/sec. The observed spectra were fitted to machine-computed Lorentzians. The temperature in the furnace or in the cryostat could be maintained within ±2 °C. A constant-velocity drive described earlier[11] was used to impart velocity to the absorber. The positive velocity in the Mössbauer spectrum corresponds to the absorber moving away from the source.

III. RESULTS

X-ray diffraction patterns of $La_{1-x}Sr_xCoO_3$ compounds were indexed on a hexagonal as well as on a rhombohedral basis. The resulting data are shown in Fig. 1. All the compositions except $x=0.5$ show a slight rhombohedral distortion. Although the x-ray data on some of the samples have been described in the literature,[4,9] no detailed data for the entire range of compositions are available. The hexagonal c axis (c_H) as well as the rhombohedral angle α_R show, as a function of x, discontinuities around $x=0.125$. Similar discontinuities in c_H and α_R have also been reported by Raccah and Goodenough.[9] It is interesting that around about this very composition the paramagnetic Curie temperature Θ [$\chi = C/(T-\Theta)$] changes sign from a negative value at lower Sr concentration to a positive value for x greater than 0.125. The hexagonal a_H and the rhombohedral a_R do not show any discontinuity, although a definite decrease is seen beyond $x=0.2$. Similarly, there is no visible discontinuity in the unit-cell volume, but around $x=0.2$ there seems to be a change in the slope from a slightly positive value to a slightly negative value. All these results are consistent with a change at $x \approx 0.125$ from isolated magnetic islands in a paramagnetic host to paramagnetic islands in a ferromagnetic host. Moreover, the rhombohedral distortion decreases with increasing Sr content, and $La_{0.5}Sr_{0.5}CoO_3$ appears to be perfectly cubic.

Differential-thermal-analysis curves of $LaCoO_3$ show three endothermic peaks at 680, 900, and 1210 K, respectively.[1] Of these, the peak at 680 K is associated with the $R\bar{3}c \rightarrow R\bar{3}$ symmetry change, which we presume reflects an ordering of the low-spin and high-spin trivalent cobalt ions, whereas the peak at 1210 K is due to the $e_g \rightarrow \sigma^*$ phase transition.[1,2] In $La_{1-x}Sr_xCoO_3$, we see a weak endothermic peak for $x=0.01$ at 680 K; however, the transition is undoubtedly of second or higher order. We do not see this transition when $x>0.05$, indicating that the transition, if it exists at all, should be of higher order. It is interesting that the plateau in the χ^{-1} vs T curve, which signifies the change in the symmetry from $R\bar{3}c$ to $R\bar{3}$ in $LaCoO_3$, is also not seen when x is greater than 0.05 (Fig. 2). The endothermic peaks in the DTA curves, corresponding to the $e_g \rightarrow \sigma^*$ electron transition at 1210 K, can be clearly seen up to $x=0.2$. The ΔH corresponding to this transition decreases with increasing x, the transition being hardly visible beyond $x=0.2$. The ΔH of the transition for $x=0.125$ is 350± 100 cal/mole as compared to 1 kcal/mole in pure $LaCoO_3$.

Electrical-resistivity data on some of the $La_{1-x}Sr_xCoO_3$ compounds were reported quite some time ago by Gerthsen and Hardtl[12]; data on $La_{0.5}Sr_{0.5}CoO_3$ were reported by Watanabe[13] and more recently by Menyuk, Raccah, and Dwight.[14]

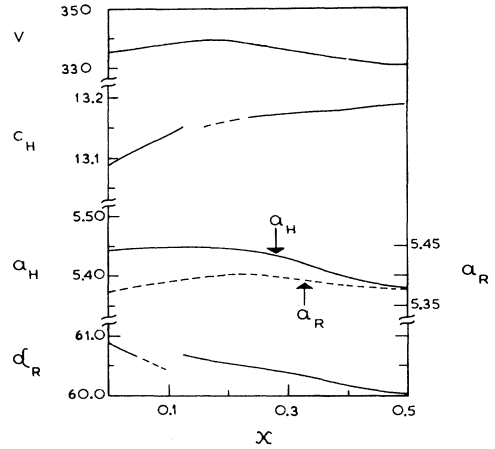

FIG. 1. Hexagonal and rhombohedral parameters for various compositions. Also shown is the unit-cell volume for different compositions.

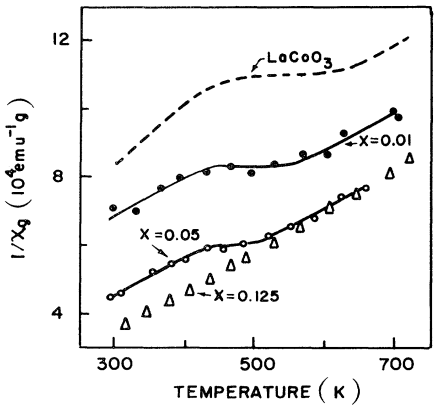

FIG. 2. Plot of reciprocal susceptibility vs temperature for different compositions.

We have carried out detailed resistivity measurements over the entire range of compositions ($0.01 \leq x \leq 0.5$) in the temperature range 78–1300 K. The resistivity data between 300 and 1300 K are shown in Fig. 3. For x up to 0.05, the behavior of $La_{1-x}Sr_xCoO_3$ is similar to that of $LaCoO_3$ in the entire temperature range studied. Just as in $LaCoO_3$, the resistivity data for compositions with $x < 0.05$ show a break around 200 K with an activation energy less than or equal to 0.1 eV in the lower-temperature region. This activation energy probably corresponds to the promotion of a t_{2g} electron to an acceptor level. For $x \geq 0.125$, the nature of the resistivity changes with temperature are different from those observed in $LaCoO_3$. For $x = 0.125$–0.4, the resistivity slightly decreases with temperature. In fact, for $x = 0.4$, the resistivity is practically independent of temperature within the range 250–600 K. For $x = 0.5$ the resistivity increases with temperature, indicating metallic behavior. These variations in electrical resistivity, from semiconductor behavior in $LaCoO_3$ to metallic behavior in $La_{0.5}Sr_{0.5}CoO_3$, are also reflected in the Seebeck-coefficient data. The Seebeck coefficient α (Fig. 4) decreases markedly around 400 K in $La_{1-x}Sr_xCoO_3$ with $x < 0.125$. In the temperature range 400–1200 K, the Seebeck coefficient decreases slightly with temperature. For $x > 0.125$, α increases linearly with T over the entire temperature range, indicating metallic behavior.

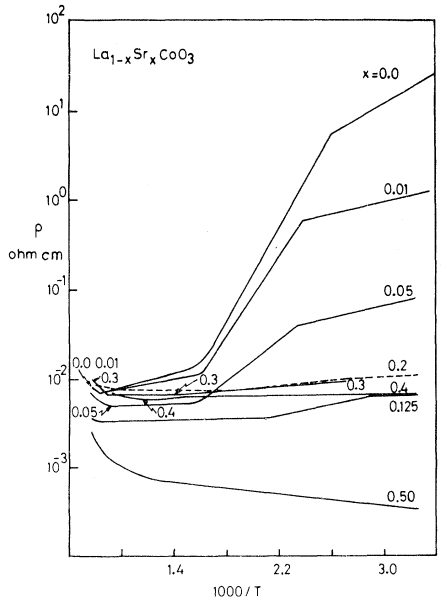

FIG. 3. Plot of logarithm of electrical resistivity ρ vs reciprocal of absolute temperature for different compositions.

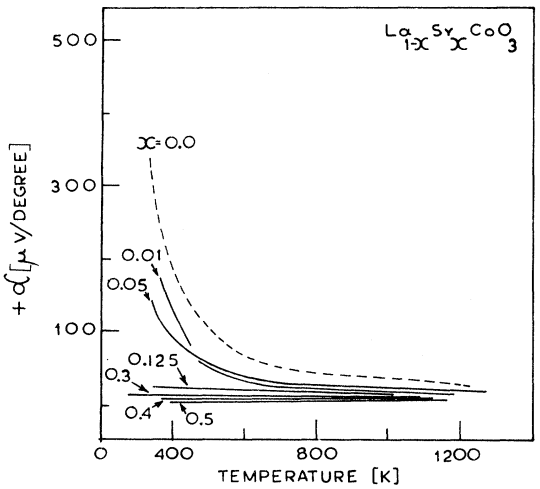

FIG. 4. Variation of Seebeck coefficient with temperature for different compositions.

In view of the metallic behavior exhibited by $La_{0.5}Sr_{0.5}CoO_3$, reflectance data were obtained for this composition. The reflectance data show a minimum around 2.30 eV. We believe that this marks the plasma frequency in this metal. The plasma frequency ω_p is related to the conductivity σ through the equation

$$\omega_p^2 = \sigma/\epsilon_\infty \tau \ ,$$

where τ is the relaxation time, ϵ_∞ is the optical dielectric constant. It is instructive to compare the location of this plasma frequency with that in other metals. In silver and ReO_3 (which is comparable to copper in electrical conductivity) the plasma frequencies are at 4.0 and 2.3 eV, respectively.[15] In TiO, the plasma frequency is found at 3.8 eV.[16] The plasma frequency in $La_{1-x}Sr_xCoO_3$ apparently shifts to higher energies as x decreases from 0.5 to 0.4.

Figure 5 shows typical Mössbauer spectra at room temperature for various compositions $La_{1-x}Sr_xCoO_3$ ($0 < x \leq 0.5$) matched against a $K_4Fe(CN)_6 \cdot 3H_2O$ single-crystal absorber. For reference, we also show the spectra for $LaCoO_3$ and for nominal $SrCoO_3$. In the $SrCoO_3$ spectrum, one sees two distinct peaks located at 0.025 ± 0.04 and 0.55 ± 0.04 mm/sec, respectively. These peak positions agree very well with the peaks observed[17,18] in $SrFeO_3$ used as an absorber. It is extremely difficult to get a truly stoichiometric $SrCoO_3$ sample, and one expects, in addition to the normally expected tetravalent cobalt, some amount of trivalent cobalt. $SrFeO_3$ also is rarely stoichiometric; and in order to compensate for the oxygen deficiency, some amount (depending upon the deviation from stoichiometry) of tri-

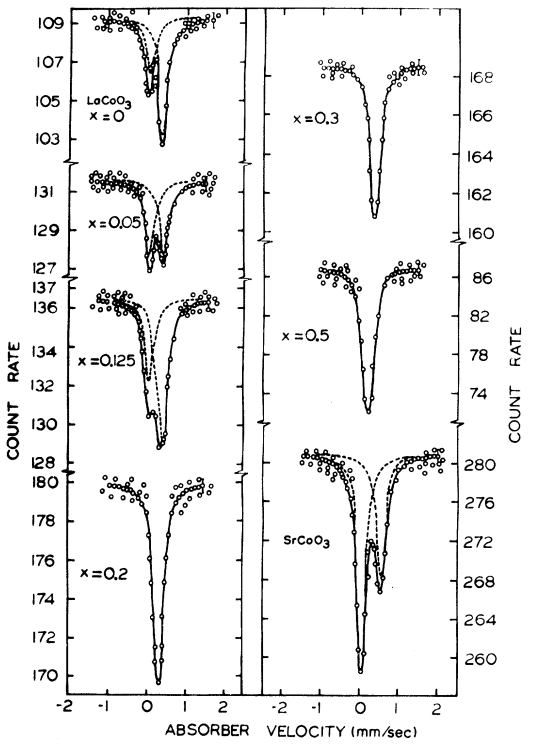

FIG. 5. Typical Mössbauer spectra of $LaCoO_3$, $La_{1-x}Sr_xCoO_3$ ($0 \leq x \leq 0.5$), and nominal $SrCoO_3$ sources at room temperature when matched against $K_4Fe(Cn)_6 \cdot 3H_2O$ single-crystal absorbers.

valent high-spin iron is created. By comparing the $SrCoO_3$ Mössbauer spectrum with that of $SrFeO_3$ and by using the isomer-shift systematics, it is easy to attribute the high-velocity resonance in the $SrCoO_3$ spectrum as arising out of high-spin trivalent iron resulting from the electron-capture decay of high-spin trivalent cobalt. The low-velocity peak is attributed to the tetravalent iron arising out of the tetravalent cobalt in $SrCoO_3$. As shown previously,[1] the two peaks in the low-temperature spectrum of $LaCoO_3$ can be uniquely assigned to high-spin Fe^{3+} ions [arising out of high-spin $Co^{3+}(t_{2g}^4 e_g^2)$ions] and low-spin Fe^{III} ions [arising out of low-spin Co^{III} $(t_{2g}^6 e_g^0)$ ions]. Only at higher temperatures, where an e_g-electron transfer creates $Co^{3+} + Co^{III} \rightarrow$ intermediate-spin tetravalent $Co(t_{2g}^4 e_g^1) + Co^{II}(t_{2g}^6 e_g^1)$ pairs, is there ambiguity in assigning the lower-velocity resonance.

Substitution of a La^{3+} ion by a Sr^{2+} ion removes a $3d$ electron from the cobalt array. The mobile hole thus created may be localized as a small polaron to make an identifiable tetravalent cobalt ion, or it may be trapped in a molecular-cluster-acceptor orbital centered at the Sr^{2+}-ion impurity. If the time it takes for a small polaron hole to jump from one cobalt ion to another is long compared to the lifetime of the excited nuclear state, the Mössbauer emission should distinguish ions of two different valence states. On the other hand, where molecular cluster or itinerant orbitals are formed, the Mössbauer emission reflects the time-averaged electronic configuration. The room-temperature Mössbauer spectra of the system $La_{1-x}Sr_xCoO_3$, $0 \leq x \leq 0.5$, exhibit two peaks if $x \leq 0.125$ and only one peak if $x > 0.125$. At $x = 0.125$, a single broad peak may be resolved into two peaks as indicated in Fig. 5.

Observation of only a single peak, located at 0.20–0.30(± 0.04) mm/sec, over the compositional range $0.125 < x \leq 0.5$ provides direct evidence for itinerant-electron formation. All efforts to find any evidence for the presence of two peaks of distinguishable tetravalent and high-spin trivalent iron failed. It is pertinent to note that the isomer shift of the single peak lies between that characteristic of high-spin Fe^{3+} and of low-spin tetravalent iron. The location of the single peak between the two resonances observed at lower concentrations is similar to that found in the $La_{1-x}Sr_xFeO_3$ system[18] for $x > 0.4$. The isomer shift is between that of high-spin Fe^{3+} and low-spin Fe^{IV} ions. The observation of a single resonance with a time-averaged electronic configuration in samples with $x > 0.125$ implies that the $3d$ hole is mobile and provides direct evidence for the formation of the impurity band.

Mössbauer spectra of $La_{1-x}Sr_xCoO_3$ with $x \leq 0.125$ compositions show two resonances almost at the same position as those in $LaCoO_3$, except that the low-velocity resonance is slightly broader than the high-velocity resonance. The increased width of the low-energy resonance may be due to the superposition of tetravalent iron resonance (arising because of the tetravalent cobalt formed as a result of Sr doping) on the low-spin trivalent iron resonance. As one goes from $LaCoO_3$ to $La_{1-x}Sr_xCoO_3$ with increasing x up to 0.125, the intensity ratio of the higher-velocity resonance to the lower-velocity resonance decreases up to 0.05 beyond which the ratio increases with increasing broadening on the lower-energy side of the low-velocity resonance. This suggests that as the Sr^{2+} concentration increases from $x = 0$ to $x = 0.05$, the Co^{3+} ions are converted to tetravalent cobalt. However, for $x > 0.05$, one finds a preferential conversion of Co^{III} into tetravalent cobalt.

Figure 6 shows Mössbauer spectra for various compositions at 78 K when matched against either a $K_4Fe(CN)_6 \cdot 3H_2O$ single-crystal absorber or a 310-ESS absorber. For compositions up to $x = 0.125$, the spectra at 78 K correspond closely

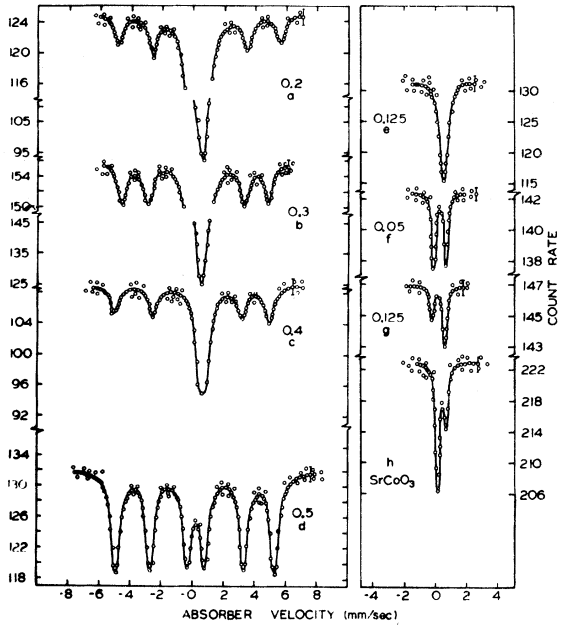

FIG. 6. Mössbauer spectra for various compositions at 78 K. (a)–(e): matched against type-310 enriched-stainless-steel absorber (ESS); (f)–(h): matched against $K_4Fe(CN)_6 \cdot 3H_2O$ absorber.

with those at room temperature except for a slight thermal shift. However, for compositions with $x \geq 0.2$ one sees the emergence of a magnetically split spectrum against the background of the paramagnetic single-line spectrum. As the Sr^{2+} content increases, the magnetically split spectrum gains in intensity at the cost of the single-line spectrum. Further, the magnetically split spectrum is observed at compositions for which the paramagnetic Curie temperature is positive. It is also interesting to note that only for those compositions that exhibit a single-line spectrum at room temperature does one observe a magnetically split spectrum.

In order to investigate the magnetic ordering further, we followed the temperature dependence of the Mössbauer spectra. Figure 7 shows the Mössbauer spectra for $La_{0.5}Sr_{0.5}CoO_3$ at various temperatures. As the temperature increases, the hyperfine-split spectrum collapses both in intensity and spacing and the paramagentic spectrum increases in intensity. Finally, above 230 K the magnetically split spectrum disappears completely. The hyperfine (hf) field at 78 K for $x = 0.5$ is 316 ± 10 kOe. The Curie temperature for this composition was determined by monitoring the disappearance of the hf field (Fig. 8). Alternately, the Curie temperature can be located by studying the variation of the area under resonance as a function of temperature. In Fig. 9 we have plotted the temperature dependence of the area under resonance. It is seen that the area under resonance decreases sharply around about 220 K, beyond which it remains practically constant. The Curie temperature determined through the disappearance of the hf field agrees closely with that determined from the variation of the area under resonance with tem-

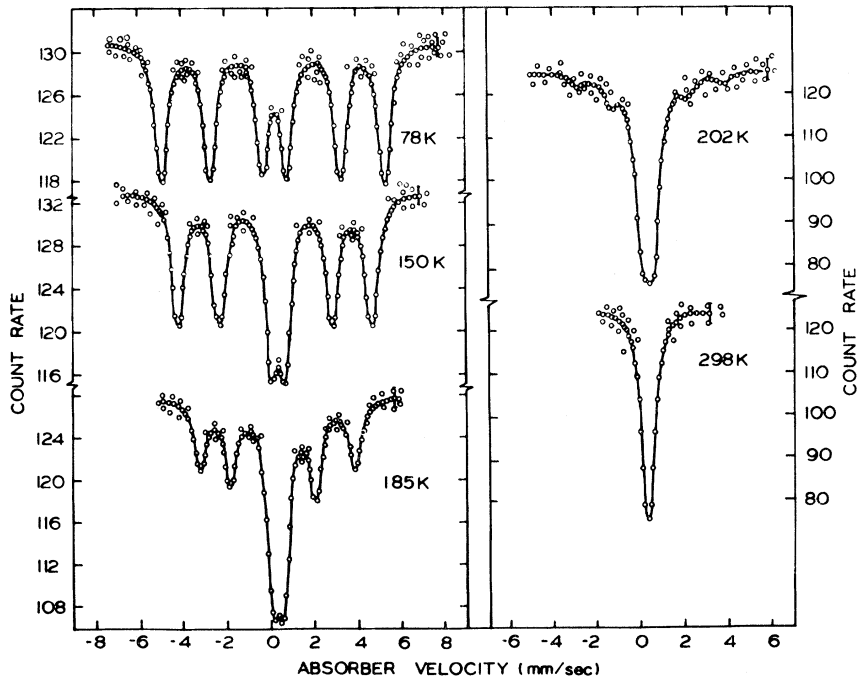

FIG. 7. Mössbauer spectra of $La_{0.5}Sr_{0.5}CoO_3$:^{57}Co source matched against 310-ESS absorber at various temperatures.

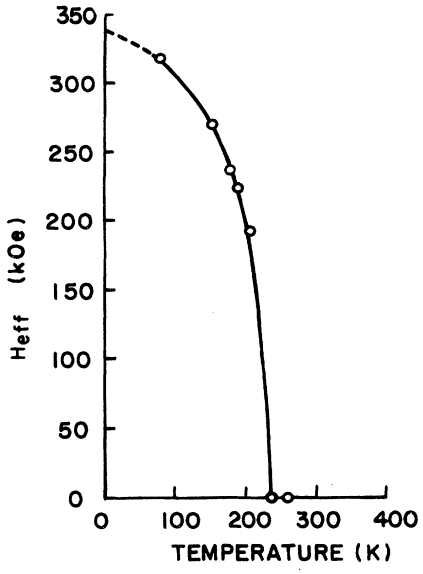

FIG. 8. Variation with temperature of the hyperfine field at the ^{57}Fe nucleus in $La_{0.5}Sr_{0.5}CoO_3$.

perature ($T_C = 230 \pm 2$ K). It is striking to note that the Curie temperature determined through Mössbauer measurements agrees remarkably closely with that determined through the gross-magnetization experiments of Raccah and Goodenough[9] and of Menyuk, Raccah, and Dwight.[14] The Curie temperature for various compositions is lower than the corresponding paramagnetic Curie temperature, especially in the range $0.15 \leq x \leq 0.45$.[9]

The hf field observed for various compositions is practically constant within experimental error. Thus at 78 K the hf field for $x = 0.5$ is $H_n = 316 \pm 20$ kOe; for $x = 0.4$, $H_n = 320 \pm 20$ kOe; and for $x = 0.3$, $H_n = 291 \pm 20$ kOe. It may be noted that the value of this hf field lies inbetween that characteristic of Fe^{3+} and of Fe^{IV}. For $x = 0.5$, the extrapolated value of the hf field at 0 K is 340 kOe. The normalized hf field at the nucleus, $H_n(T)/H_n(0)$, is plotted as a function of reduced temperature T/T_C in Fig. 10. Since the hf field at the nucleus is proportional to the saturation magnetization through Marshall's equation, $H_n = A\sigma_s$, we plot on the same curve, reduced spontaneous magnetization as a function of T/T_C. The values of saturation magnetization are from Watanabe.[13] Although the two variations agree fairly closely, this agreement should not be taken too seriously because neither H_n nor σ_s have been reduced to constant volume. The saturation magnetization in a molecular-field approximation has a temperature dependence given by

$$\frac{\sigma_s(T)}{\sigma_s(0)} = B_s\left(\frac{3S}{S+1}\,\frac{\sigma_s(T)/\sigma_s(0)}{t}\right),$$

where $t = T/T_C$ is the reduced temperature. The Brillouin function for the case $S = \frac{3}{2}$ is also shown in the same figure. Although the temperature variation of the Brillouin function agrees fairly closely with the observed variation of $H_n(T)/H_n(0)$ and $\sigma(T)/\sigma(0)$, the experimental points are below the Brillouin function in the range $0.3 \leq t \leq 0.5$, and above it in the range $0.8 \leq t \leq 1$. The fairly close agreement between the Brillouin function and the experimental points rules out the possibility of a significant biquadratic-exchange interaction. The absence of biquadratic exchange was

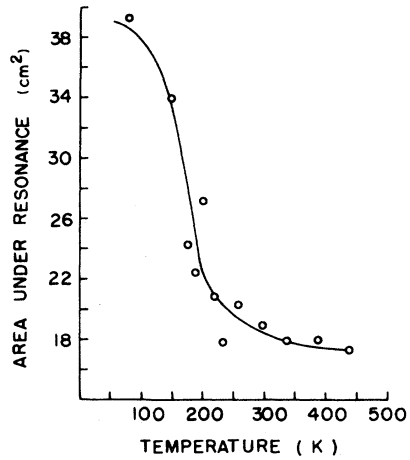

FIG. 9. Temperature variation of the area under resonance. Source $La_{0.5}Sr_{0.5}CoO_3$:^{57}Co; absorber 310 ESS.

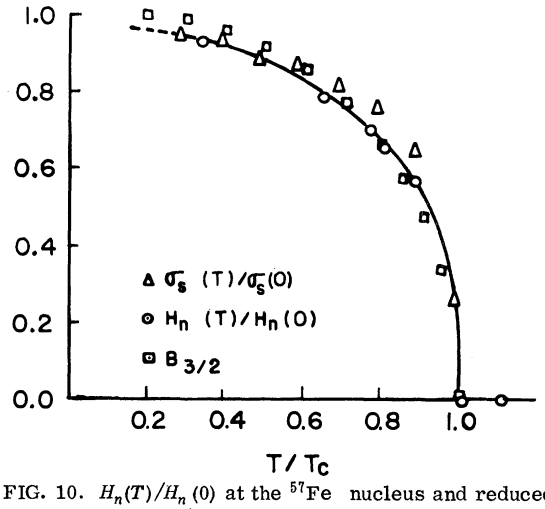

FIG. 10. $H_n(T)/H_n(0)$ at the ^{57}Fe nucleus and reduced magnetization $\sigma_s(T)/\sigma_s(0)$ as a function of reduced temperature T/T_C. Brillouin function for $S = \frac{3}{2}$ is also shown.

also reported by Menyuk *et al.*[14]

Menyuk *et al.*[14] studied the behavior of $La_{0.5}Sr_{0.5}CoO_3$ in the region of the critical temperature. They found that the critical exponent γ in the expression $\chi^{-1} \propto (T - T_C)^{\gamma}$ has a value 1.27, significantly lower than the value expected theoretically.[19,20] We also studied the behavior of this material in the vicinity of the Curie temperature. The saturation magnetization, and hence the hyperfine field, can be expressed by the following relation:

$$\frac{H_n(T)}{H_n(0)} = \frac{\sigma_s(T)}{\sigma_s(0)} = D(1 - t)^{\beta} .$$

Here D is a factor nearly unity and represents the misfit between the expression and the behavior of a real substance at 0 K. In Fig. 11, we plot $\log_{10} H_{\text{eff}}$ against $\log_{10}(1 - t)$ in the range $0.34 \leq t \leq 0.956$. From this we obtain $\beta = 0.361 \pm 0.02$ and $D = 1.171$. This value of β is close to that reported for $CrBr_3$ (0.365 ± 0.05),[21] FeF_3 (0.352 ± 0.005),[22] and the orthoferrites (0.348).[23]

IV. DISCUSSION

Our most important observations on the system $La_{1-x}Sr_xCoO_3$ are the following.

(i) In the interval $x \leq 0.125$, the paramagnetic Mössbauer spectra resolve into two resonances, which can be assigned to the different spin or valence states of iron arising out of the corresponding states of cobalt.

(ii) At no values of x in the solid-solution interval $0.125 < x \leq 0.5$, did we observe a Mössbauer resonance that could be uniquely identified as belonging to tri- and tetravalent iron. Indeed, at all temperatures the spectra could be identified to a valence state lying in between Fe^{3+} and Fe^{IV} (arising out of Co^{3+} and tetravalent cobalt).

(iii) Compositions in the interval $0.125 \leq x \leq 0.5$ exhibit a ferromagnetic component at low temperatures. The Mössbauer spectra give a single six-finger pattern at 78 K with a hf field of 320 $\pm$ 20 kOe and an isomer shift of 0.25 ± 0.04 mm/sec (relative to 310 ESS) against a background of a paramagnetic line with the same isomer shift. The values of the hf field and the isomer shift are intermediate between those for high-spin trivalent iron, Fe^{3+} ($H_n = 500$–560 kOe; isomer shift, equal to 0.40–0.60 mm/sec with respect to 310 ESS[23-26]) and low-spin tetravalent iron, Fe^{IV} ($H_n = 250$–300 kOe; isomer shift equal to -0.03–0.20 mm/sec with respect to 310 ESS[27]). These observations lead us to conclude that the Mössbauer probe "sees" a chemical environment inbetween that of high-spin Fe^{3+} and low-spin Fe^{IV} (arising out of Co^{3+} and low-spin tetravalent cobalt, respectively). A similar situation has been reported for magnetite by Ito, Ono, and Ishikawa.[28]

(iv) Above T_C, the ferromagnetic compositions give a single-line Mössbauer spectrum with an isomer shift corresponding to a chemical state inbetween Fe^{3+} and Fe^{IV}.

(v) The ferromagnetic compositions with $0.125 \leq x \leq 0.5$ exhibit a paramagnetic peak as well as a magnetically split spectrum below T_C and the area under the paramagnetic peak relative to that under the ferromagnetic peaks increases with decreasing x and with increasing temperature. Figure 12 shows the variation with temperature

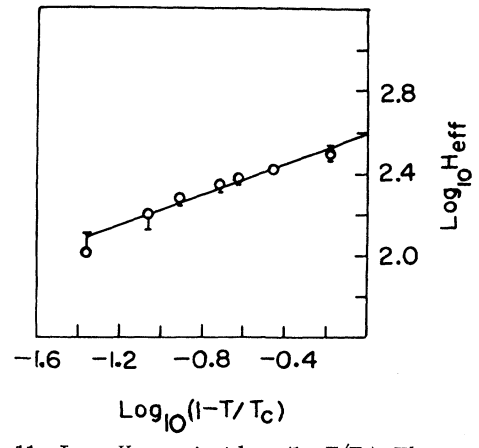

FIG. 11. $\text{Log}_{10} H_{\text{eff}}$ against $\log_{10}(1 - T/T_C)$. The error in the measurement of effective magnetic field at various temperatures is also indicated.

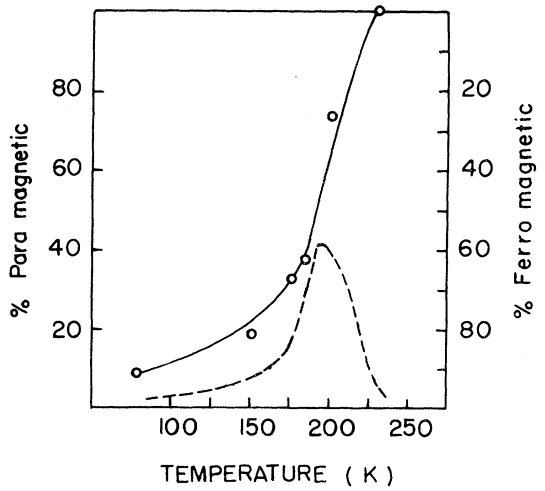

FIG. 12. Variation of paramagnetic and ferromagnetic proportions in $La_{0.5}Sr_{0.5}CoO_3$ as a function of temperature. The dotted line is the derivative of the above variation and gives the ferromagnetic-cluster-size distribution in arbitrary units.

of the percent paramagnetic area in $La_{0.5}Sr_{0.5}CoO_3$, and Fig. 13 shows the ratio of the ferromagnetic-to-paramagnetic areas at 78 K as a function x.

(vi) The existence of a sharp cutoff in the reflectivity vs energy curve indicates itinerant carriers with relatively high mobility. This observation is supported by the value and temperature coefficient of resistivity and Seebeck coefficient. It is significant to note that both the electrical conductivity and the Seebeck coefficient vary continuously through the ferromagnetic transition temperature T_C.

The ferromagnetism observed in the system $La_{1-x}Sr_xCoO_3$ could be due to one of the three mechanisms: (1) ordering of high-spin and low-spin cations through ferromagnetic superexchange inbetween them via the intervening oxygen ion,[5,6] (2) Zener double exchange,[29] and (3) itinerant-electron ferromagnetism.[9,30]

The first mechanism, based on a localized-electron model due to Anderson, was modified by Goodenough to account for the ferromagnetic interaction observed in this system. He showed that if octahedral-site magnetic cations are located on opposite sides of a common anion, they interact ferromagnetically if one cation has completely empty e_g orbitals and the other has half-filled e_g orbitals.[5] On the postulated existence of high-spin trivalent Co^{3+} and low-spin tetravalent Co^{IV}, he explained ferromagnetism in $La_{1-x}Sr_xCoO_3$ ($x > 0.125$). However, later on this mechanism was abandoned in favor of the itinerant electron ferromagnetism for the reasons indicated in the Introduction The present Mössbauer studies provide stronger evidence for abandoning the mechanism

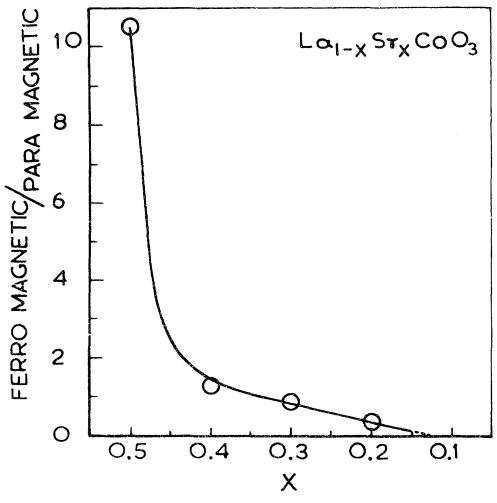

FIG. 13. Ferromagnetic to paramagnetic ratio in $La_{1-x}Sr_xCoO_3$ for various values of x.

of ferromagnetism in this system based on localized electrons. In the localized-electron configuration originally envisaged by Goodenough[5] to explain ferromagnetism in this system, the high-spin trivalent Co^{3+} transforms into high-spin divalent Co^{2+} on the transfer of a $2p$ electron into the Co^{3+} overlapping orbital. Similarly, the low-spin tetravalent cobalt Co^{IV} would go over to the low-spin trivalent Co^{III}. If this mechanism were operative, depending upon the relaxation time τ_R between the normal (Co^{3+} and Co^{IV}) and the excited state (Co^{2+} and Co^{III}) vis-à-vis, the Larmour precession time τ_L corresponding to the hf fields at the two sites, a Mössbauer spectrum will be observed. Thus if $\tau_R < \tau_L$, then the Mössbauer spectra below T_C would show two sets of six-finger patterns (with hf fields inbetween Fe^{3+} and Fe^{2+} and Fe^{IV} and Fe^{III}). However, if $\tau_R > \tau_L$, one would observe four sets of six-finger patterns corresponding to the fields characteristics of Fe^{3+}, Fe^{2+}, Fe^{IV}, and Fe^{III}. The observation of one six-finger pattern with one hf field inbetween that of Fe^{3+} and Fe^{IV} shows unequivocally that this mechanism is not operative.

One of the conditions to be satisfied for the Zener mechanism to operate is the existence of cations carrying charges differing by unity and occupying equivalent positions. According to Zener, the interaction is brought about by the simultaneous transfer of an electron from oxygen $2p$ orbital to the tetravalent cobalt and from trivalent cobalt to the $2p$ orbital of oxygen—a so-called double exchange. Indeed in this double-exchange process, a $3d$ hole associated with Co^{IV} is effectively transferred to the trivalent cobalt ion. The unit process would involve the change from configuration A to the configuration B (Fig. 14).

Zener drew attention to the fact that the resonance energy between configuration A and B is larger if spins are parallel. The Zener mechanism[29] was first postulated to explain ferromagnetism in manganites. It may be necessary to comment in brief on the electronic configuration of tetravalent cobalt. In $LaCoO_3$, the crystal-field splitting Δ_{cf} is almost equal to the exchange energy Δ_{ex}, with the consequence that only second-order effects determine whether a particular site has a low-spin trivalent cobalt ion or a high-spin cobalt ion. Essentially because of this rather critical situation, there is a coexistence of Co^{III} and Co^{3+} in $LaCoO_3$. Because of the higher positive charge on tetravalent cobalt ion, it is likely that for this ion $\Delta_{cf} > \Delta_{ex}$, ruling out the possibility of high-spin tetravalent cobalt. The resonance energy between the configurations A and B would be maximum if tetravalent cobalt has an intermediate-spin state $Co(t_{2g}^4 e_g^1)$. In this case, when double exchange takes

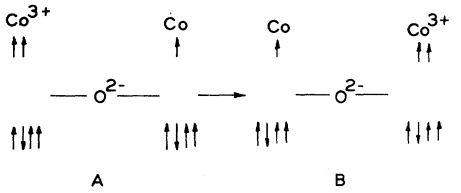

FIG. 14. Co designates an intermediate-spin cobalt state neither Co^{4+} nor Co^{IV}.

place, there is a dynamic variation in the electronic configuration of cobalt ions at both the sites between Co^{3+} and intermediate-spin tetravalent Co. This intermediate-spin tetravalent cobalt ion, on electron capture, will give low-spin tetravalent iron ion Fe^{IV}. It may be interesting to see what Mössbauer spectrum is expected on this mechanism. If the relaxation time τ_R of the transformation $Co^{3+} \rightarrow$ intermediate-spin tetravalent Co is less than the Larmour-precession time corresponding to the hf field at the site, then one would observe a single set of six-finger patterns with an hf field and isomer shift inbetween that of Fe^{3+} and Fe^{IV}. Conversely, if $\tau_R > \tau_L$, then one should observe below the transition temperature two distinct sets of six-finger patterns with hf field characteristic of Fe^{3+} and Fe^{IV}. The observation of one set of six-finger patterns with a hf field and isomer shift inbetween that characteristic of Fe^{3+} and Fe^{IV} would tend to support the Zener mechanism with the relaxation time $\tau_R < \tau_L$.

Although Mössbauer studies of this system can be explained on the basis of the Zener double-exchange mechanism, there are several other observations which unambiguously show that the Zener mechanism is not operative. Thus if the Zener mechanism were involved, there should have been a break in the electrical conductivity at T_C either because of the formation of magnetic polaron or critical scattering in the vicinity of T_C. Experimental evidence is unambiguous in that there is no discontinuity either in electrical conductivity or Seebeck coefficient.

It is possible to harmonize Mössbauer studies and electrical measurements only on the basis of itinerant-electron ferromagnetism.

The itinerant-electron model proposed by Goodenough[9,30] is summarized in Figs. 15 and 16, which show schematically the cobalt $3d$ bands for small and large x. At $T = 0$ K and small x, a narrow π^* band (formed from the crystal-field d orbitals of t_{2g} symmetry) is filled. The cobalt atoms nearest neighbor to a Sr^{2+} ion provide molecular d orbitals, those formed from atomic t_{2g} or e_g orbitals having about the same deep acceptor energy level. Thermal excitation to the high-spin

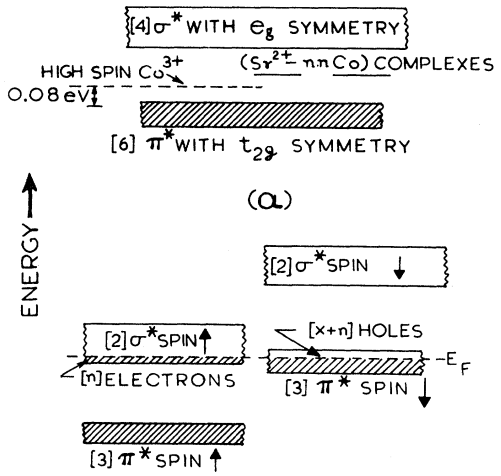

FIG. 15. (a) Cobalt $3d$ bands for La-rich region showing the Sr^{2+} impurity level; (b) cobalt $3d$ bands for ferromagnetic $La_{0.5}Sr_{0.5}CoO_3$ if no correlation splitting of π^* bands (after Goodenough, Ref. 9.)

$Co^{3+}(t_{2g}^4 e_g^2)$ configuration creates a magnetic ion, but it does not produce a mobile hole. Mobile holes are created by excitation of an electron from the π^* band to an acceptor level. At higher Sr^{2+}-ion concentrations x, the acceptor orbitals interact to form an impurity band. Because the high-spin (Co^{3+}) and low-spin (Co^{III}) configurations have comparable energies, the formation of impurity bands generates a spontaneous ferromagnetism having the σ^* bands of up spin overlapping the π^* bands of down spin. Because there is a critical Sr^{2+}-ion concentration for impurity band formation, which from experiment is $x_c \approx 0.125$, chemical inhomogeneities can produce interpenetrating ferromagnetic and paramagnetic domains. The coexistence of two magnetic phases within the same crystallographic phase would be most pronounced in the vicinity of the critical concentration x_c. On this model, the paramagnetic component is expected to decrease with increasing x and decreasing T, as has indeed been observed.

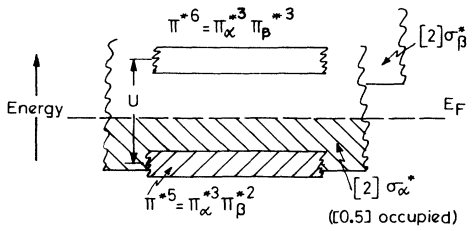

FIG. 16. Schematic cobalt $3d$ bands for ferromagnetic $La_{0.5}Sr_{0.5}CoO_3$ if the π^* bands are split by electron correlations (after Goodenough, Ref. 30.)

So long as the σ^* band remains less than one-quarter filled and the π^* band more than three-quarters filled in Fig. 15(b), itinerant-electron ferromagnetism having a Weiss constant $\Theta > T_C$ is to be anticipated. From the spontaneous magnetization of $La_{0.5}Sr_{0.5}CoO_3$ at $T = 4.2$ K

$$\mu = (x+2n)\mu_B = 1.5\mu_B ,$$

giving $n = 0.5$ for the number of up-spin σ^* electrons per molecule. Moreover, partially filled bands explain the transport and optical properties as well as the Mössbauer data.

Thus for $x < 0.1$, where Fig. 15(a) applies, one should expect two distinct valence states of cobalt: Co^{3+} and Sr^{2+} impurity-associated tetravalent cobalt along with Co^{III}, which is normally present in $LaCoO_3$. In conformity with this expectation, the Mössbauer spectra for this concentration range show two distinct resonances: a lower-velocity resonance corresponding to low-spin ions (low-spin trivalent iron and/or tetravalent iron) associated with a Sr^{2+} impurity and a higher-velocity resonance arising out of high-spin trivalent Fe^{3+} (arising out of high-spin Co^{3+}). Since the isomer shift for the low-spin trivalent and low-spin tetravalent iron differ only slightly, one gets a single resonance but with slightly higher width. So long as the Sr^{2+} ions are isolated ($x < 0.05$), the ground acceptor states appear to be doublets formed from t_{2g} orbitals of the π^* band. However, the apparent increase with x in the amplitude of the paramagnetic high-spin peak for $x > 0.05$ seems to signal the formation of magnetic clusters formed by interaction between Sr^{2+} ion impurity centers. These interactions lead to the formation of an impurity band and initiation of itinerant-electron ferromagnetism in small pockets essentially in Sr^{2+}-ion-rich regions. With further increase in Sr^{2+}-ion concentration, the ferromagnetic particle size increases and the description of Fig. 15(b) is valid. In the itinerant-electron ferromagnetic portion, the cobalt ion has a time-averaged environment inbetween that characteristic of high-spin trivalent cobalt ion and low-spin tetravalent cobalt ion. Further, this description predicts that in the neighborhood of critical concentration $x_c = 0.125$, the matrix could be adequately described as paramagnetic with few ferromagnetic particles or clusters, whereas for higher values of x reaching 0.5, the matrix is essentially ferromagnetic and metallic with small pockets of paramagnetic particles. The Mössbauer results exactly reproduce what is expected on the basis of itinerant-electron ferromagnetism. It is interesting to see that ferromagnetic particle-size distribution shifts to lower particle size with decrease in x.

The fact that $\mu = 1.5\mu_B$ in $La_{0.5}Sr_{0.5}CoO_3$ indicates the presence of $x+n \approx 1.0$ holes per molecule in the π^* bands of Fig. 15(b). That this number is essentially integral is probably not fortuitous. It suggests electron-correlation splitting of the π^{*5} and π^{*6} manifolds (as should be anticipated for the narrower π^* bands) with the Fermi energy E_F lying between them in a partially filled, overlapping σ^* band as shown schematically in Fig. 16.

In Fig. 12 we plot the ferromagnetic cluster size as a function of temperature for $La_{0.5}Sr_{0.5}CoO_3$. This analysis is based on the concept that a ferromagnetic cluster with a size less than a single domain behaves essentially as a paramagentic particle, but with a giant magnetic moment of the cluster. These so-called superparamagnetic particles have a relaxation time τ given by[31]

$$\tau = (af)^{-1} e^{KV/kT} ,$$

where a is geometric factor, K is the magnetocrystalline anisotropy constant, V is the particle volume, T is the temperature, k is Boltzmann's constant, and the frequency factor f is the Larmour frequency of the magnetization vector $\vec{M}$ in an effective field $2KV/M$. If the relaxation time of the ferromagnetic (super paramagnetic) particle is less than the nuclear Larmour precession period, then the particle will show a single-line paramagnetic spectrum. Conversely, if τ is greater than the nuclear Larmour precession period, the Mössbauer spectrum is magnetically split. Since the relaxation time depends upon both T and V, the ratio of the ferromagnetic to paramagnetic spectrum should decrease with decreasing x and increasing T as is indeed observed (Figs. 12 and 13). Figure 13 also brings out that magnetically ordered spectrum will not be observed below $x = 0.125$. Incidentally, it is at this concentration that the paramagnetic Curie temperature changes sign and around this composition we see the structural discontinuities (Fig. 1).

Since Co^{3+}-Co^{3+} interactions are antiferromagnetic (the e_g orbitals are half-filled), a Weiss constant $\Theta < 0$ is anticipated for $x < x_c$. However, for $x > x_c$ impurity band formation creates ferromagnetic domains described by Fig. 15(b) and a $\Theta > T_C > 0$ is found. The changes in the sign of Θ correlates well with the structural discontinuities found in Fig. 1 which we equate with an $x \approx x_c$.

Finally, it is interesting to compare our results with the Mössbauer studies reported[18,32] for the system $La_{1-x}Sr_xFeO_3$. The end member $LaFeO_3$ is an antiferromagnetic insulator.[23] For small x, there is only a single magnetically split spectrum at room temperature. The isomer shift changes from 0.432 to 0.580 mm/sec with increasing x. In the compositional range $0.4 \leq x \leq 0.7$, the magnetic-

ordering temperature is below 300 K and the room-temperature Mössbauer spectrum shows a single peak with an isomer shift lying inbetween that for Fe^{3+} and Fe^{IV} ions. Thus, here also electron transfer is so fast that all iron nuclei "see" the same chemical environment over the lifetime of the excited nuclear state. This observation is compatible with itinerant $3d$ holes. At higher x, distinguishable peaks can be identified with high-spin Fe^{3+} and low-spin Fe^{IV} ions. It would be interesting to relate electron-transport properties and Mössbauer studies on this system.

ACKNOWLEDGMENTS

The authors would like to thank Dr. J. B. Goodenough for helpful correspondence and discussions. One of us (D. S. R.) wishes to thank the Council of Scientific and Industrial Research for the award of Research Fellowship held during the course of this study.

[1]V. G. Bhide, D. S. Rajoria, G. Rama Rao, and C. N. R. Rao, Phys. Rev. B 6, 1021 (1972).
[2]P. M. Raccah and J. B. Goodenough, Phys. Rev. 155, 932 (1967).
[3]We prefer to assign the intermediate-spin Co state to the tetravalent cobalt, rather than the high-spin Co^{4+}; intermediate-spin tetravalent Co gives rise to low-spin Fe^{IV} on electron-capture decay.
[4]G. H. Jonker and J. H. Van Santen, Physica 19, 120 (1953).
[5]J. B. Goodenough, J. Phys. Chem. Solids 6, 287 (1958).
[6]P. W. Anderson, Phys. Rev. 79, 350 (1950); 79, 705 (1950).
[7]J. B. Goodenough, Czech. J. Phys. B 17, 304 (1967); Prog. Solid State Chem. 5, 145 (1972).
[8]C. N. R. Rao and G. V. Subba Rao, Phys. Status Solidi A 1, 597 (1970).
[9]P. M. Raccah and J. B. Goodenough, J. Appl. Phys. 39, 1209 (1968).
[10]J. B. Goodenough and P. M. Raccah, J. Appl. Phys. 36, 1031 (1965).
[11]V. G. Bhide and M. S. Multani, Phys. Rev. 139, A1983 (1965).
[12]P. Gerthsen and K. H. Hardtl, Z. Naturforsch. A 17, 514 (1962).
[13]H. Watanabe, J. Phys. Soc. Jpn. 12, 515 (1957).
[14]N. Menyuk, P. M. Raccah, and K. Dwight, Phys. Rev. 166, 510 (1968).
[15]R. Sharan, in *Modern Aspects of Solid State Chemistry*, edited by C. N. R. Rao (Plenum, New York, 1970).
[16]C. N. R. Rao, W. E. Wahnseidler, and J. M. Honig, J. Solid State Chem. 2, 315 (1970).
[17]G. Shirane, D. E. Cox, and S. L. Ruby, Phys. Rev. 125, 1158 (1962).
[18]U. Shimony and J. M. Knudsen, Phys. Rev. 144, 361 (1966).
[19]C. Domb and M. F. Sykes, Phys. Rev. 128, 168 (1962).
[20]J. Gammel, W. Marshall, and L. Morgan, Proc. R. Soc. A 275, 257 (1963).
[21]S. D. Senturia and G. B. Bendek, Phys. Rev. Lett. 17, 475 (1966).
[22]G. K. Wertheim, in *Mössbauer Effect Methodology*, edited by I. J. Gruverman (Plenum, New York, 1968), Vol. 4, p. 159.
[23]M. Eibschutz, S. Shtrikman, and D. Treves, Phys. Rev. 156, 562 (1967).
[24]O. C. Kistner and A. W. Sunyar, Phys. Rev. Lett. 4, 412 (1960).
[25]R. Bauminger, S. G. Cohen, A. Marinov, and S. Ofer, Phys. Rev. 122, 743 (1961).
[26]G. K. Wertheim, Phys. Rev. 124, 764 (1961).
[27]P. K. Gallagher, J. B. MacChesney, and D. N. E. Buchanan, J. Chem. Phys. 41, 2429 (1964); 43, 516 (1965).
[28]A. Ito, K. Ono, and Y. Ishikawa, J. Phys. Soc. Jpn. 18, 1465 (1963).
[29]C. L. Zener, Phys. Rev. 82, 403 (1951).
[30]J. B. Goodenough, Mater. Res. Bull. 6, 967 (1971).
[31]W. Kundig, H. Bommel, G. Constabaris, and R. H. Lindquist, Phys. Rev. 142, 327 (1966).
[32]P. K. Gallagher and J. B. MacChesney, *Faraday Symposium on Mössbauer Effect* (Faraday Society, London, 1967).